April 27-29
ETH Zurich
2015
International Workshop on
Sediment Bypass Tunnels

Saltation-abrasion model for hydraulic structures

Christian Auel, Ismail Albayrak, Tetsuya Sumi, Robert M. Boes

Abstract

The derivation of an abrasion prediction model for concrete hydraulic structures valid in supercritical flows is presented herein. The *state of the art* saltation-abrasion model from Sklar and Dietrich (2004) is modified using the findings of a recent research project on the design and layout of sediment bypass tunnels. The model correlates the impacting parameters with the invert material properties by an abrasion coefficient k_v. The value of this coefficient is verified by a similarity analysis to bedrock abrasion in river systems applying a correlation between the abrasion rate and the bed material strength. A sensitivity analysis reveals that the saltation-abrasion model is highly dependent on an adequate estimation of k_v. However, as a first order estimate the proposed model enables the practical engineer to estimate abrasion at hydraulic structures prone to supercritical flows.

Zusammenfassung

In diesem Beitrag wird ein Abrasionsvorhersagemodell für wasserbauliche Anlagen vorgestellt, die hohen Fliessgeschwindigkeiten ausgesetzt sind. Das Modell beruht auf dem Ansatz von Sklar und Dietrich (2004) und beinhaltet neue Erkenntnisse über die Partikeltrajektorien und Aufprallgeschwindigkeiten in schiessendem Abfluss. Das Modell verbindet die Einwirkungs- mit den Materialwiderstandsparametern der Sohle mit Hilfe des Abrasionskoeffizienten k_v. Der Wert dieses Koeffizienten wurde anhand einer Ähnlichkeitsanalyse zur Flusssohlenabrasion durch eine Korrelation der Abrasionsrate mit der Sohlmaterialfestigkeit verifiziert. Eine Sensitivitätsanalyse zeigt den grossen Einfluss dieses Parameters auf die Abrasion auf. Dennoch ist das vorgeschlagene Modell als praktische Hilfe für den Ingenieur in der Praxis geeignet, um die Abrasion an wasserbaulichen Anlagen abzuschätzen.

1 Introduction

Abrasion is a wear phenomenon involving progressive material loss due to hard particles forced against and moving along a solid surface. In bedrock rivers, abrasion is the driving process for bed incision (Sklar and Dietrich 2004, 2006, Lamb *et al.* 2008, Turowski 2009), while in hydraulic structures such as spillways, weirs, flushing channels and sediment bypass tunnels abrasion causes severe damage of the concrete invert

surface (Jacobs *et al.* 2001, Auel and Boes 2011, Helbig *et al.* 2012, Boes *et al.* 2014). In general, abrasive damage can always be expected when particle bedload transport takes place. Particles are transported in sliding, rolling or saltation motion depending on the flow conditions causing grinding, rolling or saltating impact stress on the bed. According to Bitter (1963a, b) and Sklar and Dietrich (2001, 2004) the governing process causing abrasion is saltation, whereas sliding and rolling do not cause significant wear. A number of models exist to predict the abrasion rate. While the models for prediction of bedrock incision rate (Sklar and Dietrich 2004, Lamb *et al.* 2008) focus on typical flow conditions in river systems in the sub- and low supercritical flow regime, the others for prediction of abrasion rate on concrete surfaces (Ishibashi 1983, Helbig and Horlacher 2007) have to account for highly supercritical flows. So far, the latter are either only locally applied or only valid in a limited parameter range.

In this research paper, the widely applied *state of the art* saltation-abrasion model of Sklar and Dietrich (2004) is described and modified using results of Auel (2014) to develop a new abrasion prediction model valid for concrete abrasion in sediment-laden supercritical flows.

2 Parameter definitions

2.1 Abrasion rate

The abrasion rate is expressed either as a vertical abrasion rate, an abrasion mass or a volume. These correlations have to be conscientiously taken into account when comparing different models. The abrasion depth h_a is related to the vertical abrasion rate A_r by

$$A_r = \frac{h_a}{t} \qquad \text{[m/s]} \qquad [1]$$

where t = time. The volumetric abrasion rate A_{rv} is related to A_r by

$$A_{rv} = A_r b \qquad \text{[m}^3\text{/(sm')]} \qquad [2]$$

where b = decisive width. The gravimetric abrasion rate A_{rg} is related to A_{rv} by

$$A_{rg} = A_{rv}\rho_c \qquad \text{[kg/(sm')]} \qquad [3]$$

where ρ_c = invert material density. The gravimetric and volumetric abrasion rates are expressed per meter length [m'] of the abraded section.

2.2 Tensile and compression strength

Depending on the research field different parameters are used to describe the bed material strength in literature. In geomorphological research the bedrock abrasion is correlated to the tensile strength f_t (Sklar and Dietrich 2001, Lamb *et al.* 2008, Turowski *et al.* 2013, Scheingross *et al.* 2014), whereas in civil engineering the concrete abrasion is mostly related to the compression strength f_c (Jacobs *et al.* 2001, Mechtcherine *et al.*

2012, Helbig *et al.* 2012). In order to compare the data, the material strength parameters have to be clarified and a suitable transformation has to be done.

Three types of tensile strength tests are commonly used in engineering science: direct f_t, flexure f_{tf}, and splitting tension f_{tsp} (Arioglu *et al.* 2006). Direct tension strength is accepted as the genuine value. However, the simplest and mostly applied method is the splitting tension test. In this test, a cylindrical sample is placed between two plates in a test machine and loaded. This loading generates almost uniform tensile stress along the diameter causing the sample to fail by splitting along a vertical plane (Arioglu *et al.* 2006). The splitting tensile strength f_{tsp} is a function of the direct tensile strength f_t as

$$f_t = \alpha f_{tsp} \qquad \text{[MPa]} \qquad [4]$$

where α = correlation coefficient. The value of α is basically not constant. However, an average value of $\alpha = 0.9$ is given by Hannant *et al.* (1973) and is applied in engineering practice (CEB-FIB 1991, Arioglu *et al.* 2006).

Arioglu *et al.* (2006) found a correlation between the tensile and the compression strength based on a sound regression analysis using 30 data sets valid for $4 < f_{c,cyl} < 120$ MPa:

$$f_{tsp} = 0.387 f_{c,cyl}^{0.63} \qquad \text{[MPa]} \qquad [5]$$

Similar to the tensile strength tests, the compression strength is also derived from different test procedures. Samples are either cubed or cylindrical, and the relationship between them is given as

$$f_{c,cyl} = \beta f_{c,cube} \qquad \text{[MPa]} \qquad [6]$$

where $\beta = 0.8$ = correlation coefficient according to EN 1992-1-1.

3 Saltation-abrasion model

Sklar and Dietrich (2004) published an outstanding work by analyzing a wide range of research data sets on particle motion and abrasion and proposed a saltation-abrasion model to predict bedrock abrasion in river systems. The magnitude of abrasion is expressed as a vertical abrasion rate A_r in the following form

$$A_r = \frac{q_s W_{im}^2 Y_M}{L_p k_v f_{tsp}^2}\left(1 - \frac{q_s}{q_s^*}\right) \qquad \text{[m/s]} \qquad [7]$$

where W_{im} = mean vertical particle impact velocity [m/s], Y_M = Young's Modulus of elasticity [Pa], L_p = particle saltation length, k_v = rock resistance coefficient [-], q_s = specific gravimetric bedload rate [kg/(sm)], and q_s^* = specific gravimetric bedload transport capacity [kg/(sm)]. Note that all parameters have to be applied in SI units, thus the units of Y_M and f_{tsp} are in [Pa], not in [MPa].

The last term on the right in Eq. (1) is related to the cover effect occurring at high bedload transport rates partly or totally covering the bed, leading to a decrease in particle impact energy (Sklar and Dietrich 1998, Turowski 2009). The coefficient k_v describes the correlation between bed material and sediment properties and abrasion rate (further explanation in Section 3.3).

Sklar and Dietrich (2004) applied correlations obtained for the hop length, hop height, and particle velocity to Eq. (7) and proposed the saltation abrasion model for bedrock river abrasion in the following form:

$$A_r = \left(\frac{0.08(s-1)gY_m}{k_v f_{tsp}^2} \right) q_s \left(\frac{\theta}{\theta_c} - 1 \right)^{-0.5} \left(1 - \frac{q_s}{q_s^*} \right) \left(1 - \left(\frac{U_*}{V_s} \right)^2 \right)^{1.5} \quad \text{[m/s]} \quad [8]$$

where θ = Shields parameter calculated as $\theta = U_*^2/[(s\text{-}1)gD]$, where $s = \rho_s/\rho$, ρ_s = particle density, ρ = fluid density, D = particle diameter, $U_* = (gR_hS)^{0.5}$ = friction velocity, g = gravitational acceleration, R_h = hydraulic radius, S = energy line slope, and θ_c = critical Shields parameter and V_S = particle settling velocity.

3.1 Modified saltation-abrasion model

The work of Sklar and Dietrich (2004) focuses on bedrock river systems with moderate flow velocities in the sub- or slightly supercritical range. Concrete abrasion processes at hydraulic structures such as weirs, spillways, outlets and sediment bypass tunnels are often exposed to highly supercritical flows (Jacobs *et al.* 2001, Helbig and Horlacher 2007, Auel 2014). Especially sediment bypass tunnels are exposed to severe abrasion of the tunnel invert due to high flow velocities in combination with high bedload transport (Sumi *et al.* 2004, Auel and Boes 2011).

To apply the saltation-abrasion model to such conditions, Auel (2014) conducted a scaled hydraulic model study in a 13.50 m long straight laboratory flume to analyze the flow characteristics, particle motion and invert abrasion in supercritical flows. The results of flow mean and turbulence characteristics and the particle motion analysis are published in Auel *et al.* (2014a, b) and Auel (2014), respectively. The latter implies the determination of the transport mode, particle velocities and saltation trajectories for a wide range of flow velocity, flow depth, bed slope, and particle diameter. It is found that the particle saltation velocity and trajectory strongly correlate with both Froude number $\mathsf{F} = U/(gh)^{0.5}$, where U = flow velocity and h = flow depth, and Shields parameter θ.

Furthermore, Auel (2014) conducted experiments to investigate the spatial and temporal invert abrasion development using weak mortar as bed material in the hydraulic model under a range of hydraulic and particle parameters (Table 1). The compression and flexure tensile strengths were obtained from direct load tests in the laboratory and the

Young's modulus was estimated applying a formulation by Noguchi *et al.* (2009) based on more than 3000 data sets valid for a range from f_c = 40 to 160 MPa:

$$Y_M = k_1 k_2 \cdot 33500 \left(\frac{f_c}{60} \right)^{(1/3)} \left(\frac{\rho_c}{2400} \right)^2 \quad \text{[MPa]} \quad [9]$$

where k_1 and k_2 are correction factors accounting for the type of coarse aggregate and admixtures, respectively. In Auel (2014), $k_1 = k_2 = 1.0$ is chosen due to small sand aggregates (D = 1-1.4 mm) and no admixtures. Although the mortar properties were about an order of magnitude lower compared to standard concrete, they showed similar behavior in terms of curing times and material collapse characteristics at the conducted load tests.

Table 1: Mortar properties (Auel 2014)

		Hard mixture	Samples *n*	Soft mixture	Samples *n*
Water/cement ratio	[-]	0.6		0.6	
Sand/cement ratio	[-]	10		15	
$f_{c,cube}$	[MPa]	6.81 ±1.21	33	3.67 ±0.60	34
f_{tf}	[MPa]	0.84 ±0.18	14	0.56 ±0.11	13
ρ_c	[kg/m^3]	1773 ±0.58	17	1692 ±45	16
Y_M	[MPa]	9061 ±657		6723 ±454	

Based on the findings of Auel (2014) a modified saltation-abrasion model applicable for hydraulic structures prone to supercritical flows is proposed in the following form similar to Sklar and Dietrich (2004):

$$A_r = \frac{Y_M}{k_v f_{tsp}^2} W_{im}^2 \cdot I \cdot q_s \quad \text{[m/s]} \quad [10]$$

where I = number of particle impacts per unit length [1/m]. Note that similar to Eq. (7), Y_M and f_{tsp} have to be applied in [Pa]. The cover effect term in Eq. (7) is dropped due to the fact that Auel (2014) did not observe any cover tendencies in his experiments for the parameter range tested. Sklar and Dietrich (2004) developed equations for the estimation of W_{im} and L_p in Eq. (7) and implemented in Eq. (8). However, they are not applicable for saltating particles in highly supercritical flows (Auel 2014). Therefore, new equations for these terms based on Auel (2014) are introduced below for Eq. (10).

The number of impacts per unit length is defined as the reciprocal value of the hop length L_p as:

$$I = \frac{\left(1 - \left(U_* / V_s\right)^2\right)^{0.5}}{L_p} \left(1 - P_R\right) \quad \text{[1/m]} \quad [11]$$

where P_R = rolling probability. The numerator of the first term on the right hand side is proposed by Sklar and Dietrich (2004) and accounts for the mode shift from saltation to suspension. V_s may be calculated using the equation developed by either Dietrich (1982) or Ferguson and Church (2004). The rolling probability P_R and hop length L_p are given in Auel (2014).

The following further assumptions are proposed:

- $f_{tsp} = 0.387 f_{c,cyl}^{0.63}$ (Eq. 5)
- $W_{im} = U_*$
- $k_v = 10^6$

In the following, the two latter assumptions will be explained in detail.

3.2 Estimation of particle impact velocity

Motion of a saltating particle in water stream is described with a saltation trajectory of length L_p and height H_p, and particle impact velocity V_{im} at an impact angle γ_{im} (Figure 1). The vertical velocity component is given by $W_{im} = V_{im} \sin(\gamma_{im})$. As direct measurements of W_{im} or γ_{im} are scarce, Sklar and Dietrich (2004) approximate W_{im} as follows:

$$W_{im} = \frac{3 H_p V_p}{L_p} \quad \text{[m/s]} \qquad [12]$$

where V_p = average particle velocity. Sklar and Dietrich (2004) analyzed a number of particle saltation research studies in sub- and slightly supercritical flow and proposed correlations to express L_p, H_p and V_p as functions of the transport stage $T^* = \theta/\theta_c$ with $\theta_c = 0.03$.

In Auel (2014) single particles were recorded by means of a high-speed camera system. The main objective was to investigate the particle transport mode, particle velocities, saltation trajectories and the particle impact energy when a particle impinges the bed at saltation motion. The experiments were conducted at supercritical hydraulic flow conditions for a wide range of aspect ratios and Froude numbers implying in total 264 parameter variations using both natural sediment and glass spheres. The following relations were found:

$$\frac{H_p}{D} = 5.9\theta \qquad R^2 = 0.85 \qquad [13]$$

Note that in Eq. (13), H_p is defined from particle center to particle center and not from bed to center (Figure 1). The hop length follows:

$$\frac{L_p}{D} = 251\theta \qquad R^2 = 0.94 \qquad [14]$$

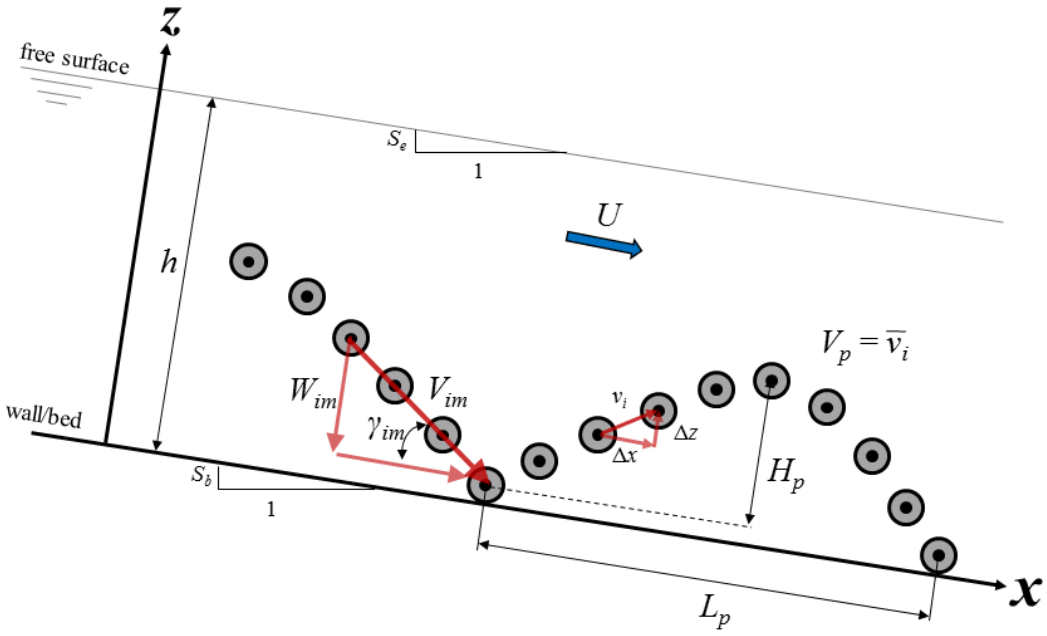

Figure 1: Sketch of saltating particle

The particle velocity V_p, defined as the average downstream travelling velocity (Figure 1), is determined by analyzing data from Auel (2014) as:

$$\frac{V_p}{\left((s-1)gD\right)^{0.5}} = 20 \cdot \theta^{0.5} \qquad R^2 = 0.98 \qquad [15]$$

The fit scales with the square root of θ, thus Eq. (15) can be simplified to

$$V_p = 20 \cdot U_* \qquad [16]$$

revealing that the particle velocity is directly related to the friction velocity by the factor 20. Applying Eqs. (13), (14) and (15) to Eq. (12) leads to the simple correlation

$$W_{im} = 1.4 \cdot U_* \qquad [17]$$

Auel (2014) obtained the particle impact velocity directly from the experimental data by averaging the particle velocities v_i over three consecutive recorded images before impact as:

$$V_{im} = \frac{v_{i-3} + v_{i-2} + v_{i-1}}{3} \qquad [18]$$

The vertical particle velocity W_{im} is identically calculated. Figure 2 shows W_{im} as a function of θ and reveals that W_{im} scales with the square root of the Shields parameter. The fit follows:

$$\frac{W_{im}}{\left(\left(s-1\right)gD\right)^{0.5}} = \theta^{0.5} \qquad R^2 = 0.75 \qquad [19]$$

and may be simplified to:

$$W_{im} = U_* \qquad [20]$$

Hence, two expressions to describe the vertical impact velocity are proposed. It is revealed that the approximation of the vertical impact velocity proposed by Sklar and Dietrich (2004) in Eq. (12) overestimates the measured data in Eq. (20) by a factor of 1.4. Carefully consider that the derivation of both vertical velocities is based on the saltation trajectory analysis in supercritical flows described in Auel (2014). Sklar and Dietrich (2004) proposed different assumptions for the saltation height, length and particle velocity. Applying these fits must not necessarily lead to the same factor of 1.4. However, as no direct W_{im} measurements are available for the data sets used in Sklar and Dietrich (2004), this cannot be definitively clarified.

It is recommended not to neglect the deviation in both derivations due to the fact that the impact velocity scales quadratically with the saltation-abrasion model. For supercritical flows, it is recommended to use the expression found in Eq. (20) to calculate the vertical impact velocity W_{im}.

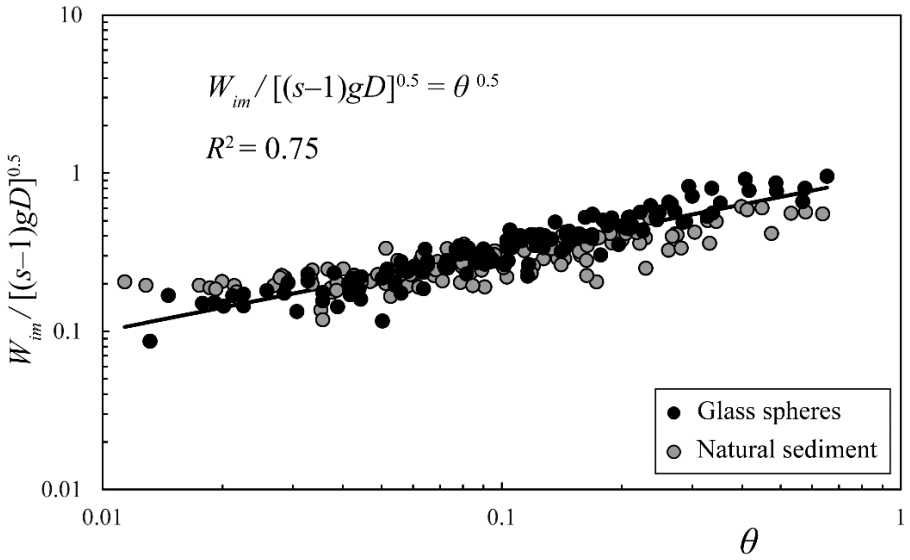

Figure 2: Vertical impact velocity W_{im} as a function of Shields parameter θ based on 264 data points from Auel (2014)

3.3 Correlation between abrasion rate and bed material properties

Sklar and Dietrich (2001) proposed a direct correlation between the material strength and the gravimetric material abrasion rate (Figure 3a). They conducted abrasion exper-

iments in an in-house-developed water-filled abrasion mill. The mill bottom was covered with the probed material. A constant amount of sediment gravel particles was added (M = 150 g, D = 6 mm) using a constant propeller stirring velocity (1000 rpm). In total, 22 rock and six concrete disc samples were tested. Due to the fact that rock exposed to saltating particle impacts fails in tension, Sklar and Dietrich (2001) selected the tensile strength as the decisive parameter. The tensile strength was obtained using the Brazilian test method, thus their values refer to the splitting tensile strength f_{tsp} (Rocco *et al.* 1999). Sklar and Dietrich (2001) proposed the following correlation (Figure 3a):

$$A_{rg} = 7.7(\pm 1.4)\, f_{tsp}^{-2(\pm 0.1)} \quad \text{[g/h]} \qquad [21]$$

Additionally they conducted single grain experiments with 70 g quartzite gravel and proposed based on 6 rock samples:

$$A_{rg} = 18(\pm 4.0)\, f_{tsp}^{-2(\pm 0.6)} \quad \text{[g/h]} \qquad [22]$$

Sklar and Dietrich (2004) used 9 single grain data sets from Sklar and Dietrich (2001) to quantify the rock resistance coefficient k_v by rearranging Eq. (8) to:

$$k_v = \left(\frac{0.08(s-1)gY_m}{f_{tsp}^2} \right) \frac{q_s}{A_r} \left(\frac{\theta}{\theta_c} - 1 \right)^{-0.5} \left(1 - \left(\frac{U_*}{V_s} \right)^2 \right)^{1.5} \qquad [23]$$

Additionally they analyzed 6 data sets from single particle drop tests. Considering both, the abrasion mill and particle drop tests, they found an average value of

- $k_v = 3.0 \times 10^6$ in a range of 1.0 to 9.0×10^6

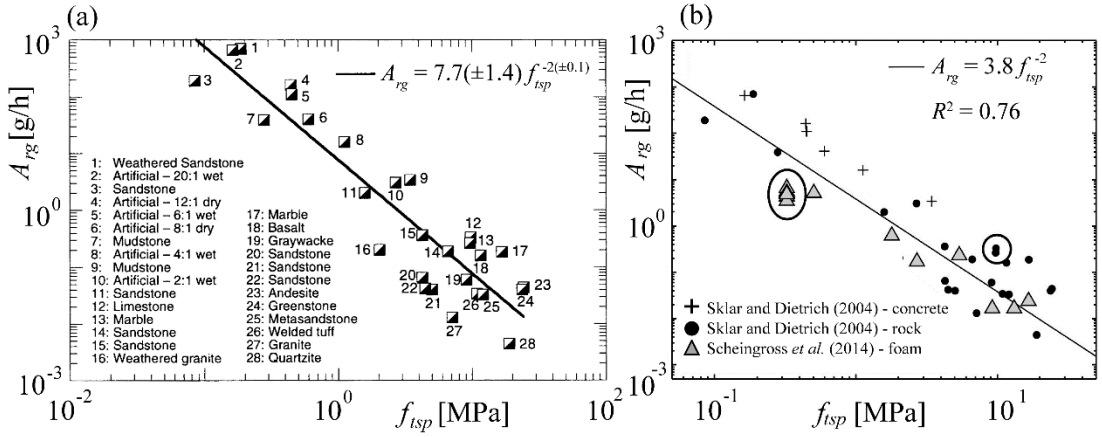

Figure 3: Abrasion mill experiments. Gravimetric abrasion rate Arg as function of splitting tensile strength ftsp from (a) Sklar and Dietrich (2001), and (b) Scheingross et al. (2014)

For application of the saltation abrasion model, they proposed to use the following estimate:

- $k_v \sim 10^6$ (Sklar and Dietrich 2004, 2012)

In order to reproduce these stated values, the abrasion mill experiment data used in Sklar and Dietrich (2004) are listed in Table 2. The average k_v value calculated from this data set is:

- $k_v = 3.6(\pm 2.5)\times 10^6$ (Table 2, Column 6)

This value slightly deviates by 0.6×10^6 from the above stated mean value given by Sklar and Dietrich (2004) due to the fact that the single particle drop tests are not considered in this calculation. Recalculation of the data, using the parameters given in Sklar and Dietrich (2004, Section 5.1: q_s = 1.08 kg/(sm), θ/θ_c = 1.2, U_*/V_s = 0.19, $Y_M = 5\times 10^4$ MPa), reveals the following value:

- $k_v = 5.1(\pm 3.9)\times 10^6$ (Table 2, Column 7)

Comparing this newly calculated k_v value with the original data set reveals a disagreement of 1.5×10^6. This deviation is unclear and not completely comprehensible.

Table 2: k_v calibration from single-grain abrasion mill tests (Sklar and Dietrich 2004, Table 4b)

Sklar and Dietrich (2004)						*New calculation*		
1	2	3	4	5	6	7	8	9
Rock type	f_t	ρ_s	A_{rg}	A_r [(1)]	k_v	k_v [(2)]	k_v [(3)]	k_v [(4)]
	[MPa]	[kg/m^3]	[g/h]	[m/s]	10^6	10^6	10^6	10^6
Concrete (20:1)	0.163	2300	215	8.69×10^{-7}	4.07	5.0	3.9	1.7
Concrete (6:1)	0.448	2300	71	2.87×10^{-7}	1.63	2.0	3.9	1.7
Concrete (4:1)	1.12	2300	5.1	2.06×10^{-8}	3.63	4.5	3.9	1.7
Sandstone	1.583	2450	2.9	1.11×10^{-8}	3.37	4.7	4.6	2.0
Graywacke	9.1	2500	0.22	8.18×10^{-10}	1.38	2.0	4.9	2.1
Limestone	9.78	2600	0.21	7.51×10^{-10}	1.30	2.0	5.4	2.3
Welded tuff	10.9	2600	0.036	1.26×10^{-10}	6.23	9.6	5.4	2.3
Quarzite	19	2600	0.008	2.86×10^{-11}	9.09	13.9	5.4	2.3
Andesite	24.4	2600	0.030	1.06×10^{-10}	1.47	2.3	5.4	2.3
Average					3.6	5.1	4.8	2.0
Standard dev.					2.5	3.9	0.7	0.3

(1) Divided by disc area of A = 0.03 m^2, (2) recalculated, (3) Eq. (21), (4) Eq. (22)

Despite the above described approach (use of single data sets), it is also reasonable to directly apply the abrasion rate – material strength fits from Sklar and Dietrich (2001) given in Eqs. (21) and (22) to Eq. (23). This attempt was not done in Sklar and Dietrich (2004), but is carried out herein. Application of Eq. (21) representing the multi-grain abrasion mill experiments leads to

- $k_v = 4.8(\pm 0.7)\times 10^6$ (Table 2, Column 8).

Application of Eq. (22), representing the single particle abrasion mill experiments, leads to

- $k_v = 2.0(\pm 0.3)\times 10^6$ (Table 2, Column 9).

From the single values listed in Table 2 (Columns 8 and 9) it is obvious that k_v only varies with the sediment particle density ρ_s as the other parameters (sediment rate, friction velocity, and Shields parameter) are not varied. Considering all above listed k_v values leads to the conclusion that the deviation is high, varying almost in one order of magnitude ($1\times 10^6 < k_v < 9\times 10^6$) with average values of $k_v \approx 2\text{-}5\times 10^6$ depending on the calculation method. This conclusion confirms the parameter range already stated by Sklar and Dietrich (2004).

Scheingross *et al.* (2014) conducted similar experiments in the same device using artificial foam as a bedrock substitute but varying the particle diameter in a wide range from D = 0.5 to 44 mm while keeping the sediment mass constant with 70 g (Figure 3b). They added their data to Sklar and Dietrich (2001) and found

$$A_{rg} = 3.8 f_{tsp}^{-2} \qquad R^2 = 0.76 \qquad \text{[g/h]} \qquad [24]$$

A_{rg} scales with the inverse of the square of f_{tsp}, being consistent with the findings of Sklar and Dietrich (2001). Note that the satisfying coefficient of determination was obtained converting the data to log-transformed values prior to fitting and not from a direct power-law fitting.

Recent experiments on concrete abrasion in an abrasion drum were performed by Mechtcherine *et al.* (2012) and Helbig *et al.* (2012). Tests were conducted using concrete plate samples exposed to a water-particle mixture at the drum base. The two-phase mixture was composed of equal parts of solid and fluid, and the drum rotated in three different velocities. Typical flow conditions in a lower, middle and upper river reach were simulated using the particle diameter/flow velocity combinations R1: D = 4.4 mm and ω = 10 rev/min, R2: D = 5.0 mm and ω = 13.5 rev/min, and R3: D = 8.0 mm and ω = 17 rev/min. The abrasion rates are calculated from the provided data and given in Table 3. Helbig *et al.* (2012) stated that the abrasion depth linearly scales with time, thus data are averaged and additionally multiplied by the sample area A = 0.09 m^2 and concrete density to obtain a gravimetric abrasion rate.

In order to validate and compare the abrasion coefficient k_v, the data from Helbig *et al.* (2012) and Auel (2014) have been added to the data sets from Sklar and Dietrich (2001) and Scheingross *et al.* (2014) presented in Figure 3. The two latter sets are divided by the abrasion mill sample area A = 0.031 m^2 to allow for comparison. Furthermore, all data are expressed per meter length to allow for comparison between the abrasion mill, drum and the straight model flume experiments.

Table 3: Gravimetric abrasion rate A_{rg} obtained from drum experiments in Helbig *et al.* (2012)

Concrete No		1	2	3	4	5	6
$f_{c,cube}$	[MPa]	53	54.4	58.6	56.6	77.7	69.5
ρ_c (*)	[kg/m^3]	2299	2588	2408	2494	2389	2416
A_{rg} R1	[g/h]	154.2	100.9	104.2	100.9	121.1	91.7
A_{rg} R2	[g/h]	435.6	260.9	365.3	255.0	271.6	210.7
A_{rg} R3	[g/h]	837.6	649.2	531.2	572.1	577.8	509.1

* the concrete densities are not published in the papers but directly given by the authors

According to Setunge *et al.* (1993) the *rock strength criterion* by Johnston (1985) describing the correlation of rock material constants to the ratio of compression to tensile strength are equally valid for high strength concrete. Consequently, the conclusion may be drawn that a conversion from tensile to compression strength and vice versa is applicable for both materials, rock and concrete. Hence, the compression strength $f_{c,cube}$ values used in Helbig *et al.* (2012) and Auel (2014) are transferred to f_{tsp} values using Eqs. (5) and (6). In Figure 4 the gravimetric abrasion rate A_{rg} is given as a function of the splitting tensile strength f_{tsp}. Auel's data adequately fit in the data range of Sklar and Dietrich (2001) and Scheingross *et al.* (2014), whereas Helbig's data deviate. The fit, excluding Helbig's data, follows:

$$A_{rg} = 316\, f_{tsp}^{-2} \qquad R^2 = 0.85 \qquad \text{[g/(hm')]} \qquad [25]$$

Identically to Scheingross *et al.* (2014) the coefficient of determination is obtained converting the data to log-transformed values prior to fitting. Direct power-law fitting leads to lower values.

Data from Helbig *et al.* (2012) and Auel (2014) show a quasi-vertical alignment in Figure 4 due to the fact that material strength variation is low ($f_{c,cube}$ = 53 to 69.5 MPa for the former and $f_{c,cube}$ = 3.7 to 6.8 MPa for the latter) compared to the wide range of the tested materials. Consider that these data sets are obtained from different test setup conditions, widely varying the flow conditions and sediment parameters. The varying abrasion rate for identical strength is therefore caused by changes in sediment supply rate, particle diameter and flow velocity. These effects cannot be adequately represented by a simple correlation between the material strength and the abrasion rate as given in Figure 4.

However, the data of Auel (2014) satisfactorily fits into the sets by Sklar and Dietrich (2001) and Scheingross *et al.* (2014) and the entire data set reveals a clear correlation of the material strength to the abrasion rate. Eq. (25) may be applied to Eq. (23) to allow for comparison with the k_v values described above. Using the hydraulic parameters given by Sklar and Dietrich (2004) leads to:

- $k_v = 3.7(\pm 0.5)\times 10^6$

This value lies in the range of the above described values derived from data provided by Sklar and Dietrich (2004). Remind that k_v varies from $1\times10^6 < k_v < 9\times10^6$. All in all, the proposed first order estimate value by Sklar and Dietrich (2004) of $k_v = 10^6$ is widely accepted and used in bedrock abrasion research (Sklar and Dietrich 2006, Lamb *et al.* 2008, Huda and Small 2014, Scheingross *et al.* 2014). Furthermore, Turowski *et al.* (2007) confirmed this value reanalyzing the data from Sklar and Dietrich (2001). Thus, the authors propose to similarly use this value in the saltation abrasion model for concrete structures while keeping in mind the large variation of the abrasion coefficient.

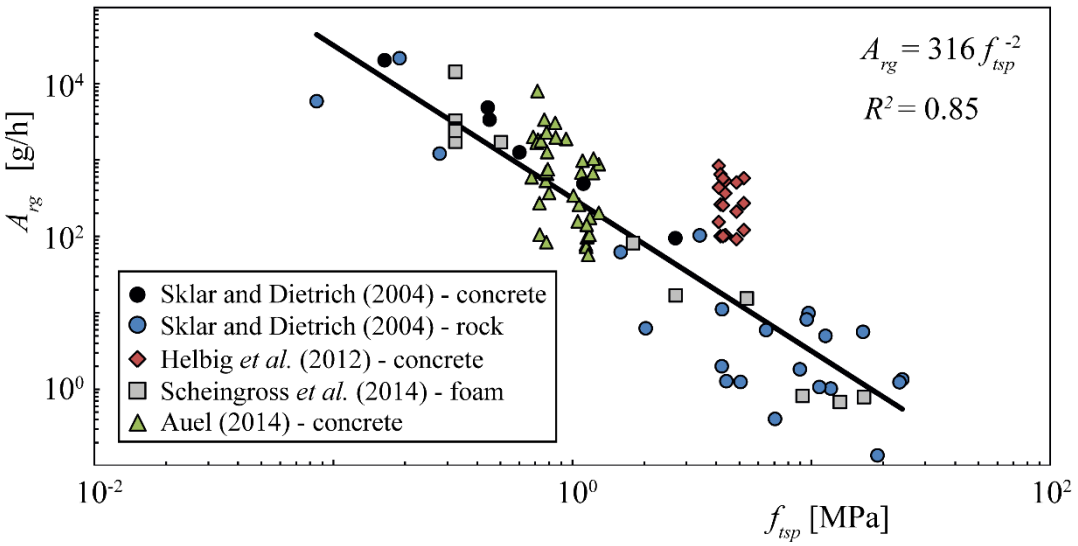

Figure 4: Gravimetric abrasion rate A_{rg} as a function of splitting tensile strength f_{tsp}. Data from Helbig *et al.* (2012) excluded from fit

4 Discussion

4.1 Sensitivity analysis

The effect of the abrasion coefficient and the vertical impact velocity on the abrasion rate given in Eq. (10) is shown in a sensitivity analysis exemplarily applying the prototype data of the Asahi sediment bypass tunnel in Japan. According to Auel (2014), the 2384 m long tunnel is b = 3.80 m wide and operated with a design discharge of Q_d = 140 m^3/s. The tunnel slope is S_b = 0.029, and the concrete invert roughness height is assumed to be k_s = 3 mm leading to a supercritical uniform flow velocity of U = 12.0 m/s and flow depth of h = 3.18 m (R_h = 1.12 m). The sediment transport rate Q_s = 1000 kg/s is randomly selected.

Figure 5 shows the abrasion rate A_r as a function of k_v, keeping all other parameters constant. For comparison, the vertical particle impact velocity is plotted as $W_{im} = 1.4\, U_*$ (Eq. 17) and $W_{im} = U_*$ (Eq. 20), the former representing the approach by Sklar and Dietrich (2004), the latter the direct data analysis, respectively (Section 3.2).

The abrasion coefficient k_v is a crucial parameter in the saltation-abrasion model. A large change of some orders of magnitude in A_r is revealed in Figure 5. Sklar and Dietrich (2004) stated that k_v is a constant based on Engel (1976), whereas Turowski *et al.* (2013) expected the parameter to be site-dependent, as it subsumes details of particle impact and rebound as well as energy-delivery processes. As discussed in Section 3.3, the coefficient varies around $k_v = 5(\pm 4)\times 10^6$. This variation causes a variation in A_r of almost one order of magnitude. Furthermore, by means of a scaling analysis, Chatanantavet and Parker (2009) stated values ranging from 10^4 for weak rocks such as weathered sandstone to 10^6 for hard rocks such as quartzite or andesite. Hence, the variation in A_r increases to some orders of magnitude leading to the conclusion that further research using standardized abrasion drum/mill facilities (Sklar and Dietrich 2001, Helbig *et al.* 2012, Scheingross *et al.* 2014) is needed to analyze in detail the effect of different bed materials such as concrete, and the effect of varying impact parameters such as flow velocity, sediment transport rate, grain size, and grain hardness.

The variation of A_r due to W_{im} is additionally presented in Figure 5. The comparison reveals that Sklar's assumption ($W_{im} = 1.4\ U_*$) almost doubles A_r. This deviation is evident as the impact velocity scales quadratically, i.e. $1.4^2 = 1.96 \approx 2$.

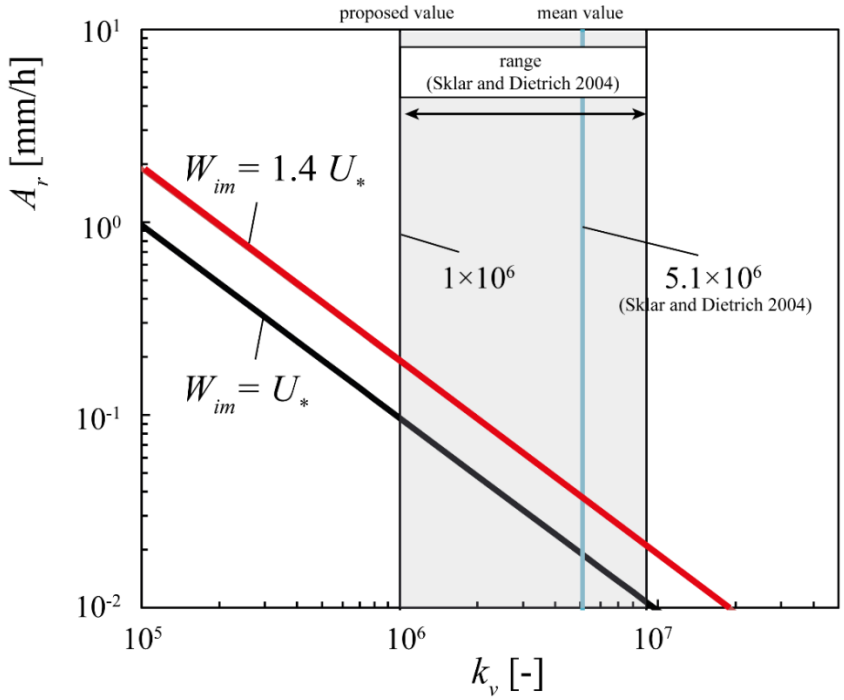

Figure 5: Vertical abrasion rate A_r based on Eq. (10) as a function of abrasion coefficient k_v. Exemplary calculation based on data of Asahi sediment bypass tunnel

4.2 Young's modulus

Based on Clark (1966), Sklar and Dietrich (2004) state that the variation in Young's modulus Y_M of rock is limited and can be treated to first order as a constant value.

Hence in bedrock abrasion related studies a constant value of $Y_M = 5\times10^4$ MPa is widely applied (Sklar and Dietrich 2004, Turowski 2007, Lamb *et al.* 2008, Huda and Small 2014). In case of concrete, the Young's modulus is not constant, but varies depending on the compression strength and particularly on the concrete density as shown for example by Noguchi *et al.* (2009) in Eq. (9). Consequently, the Young's modulus has to be studied in more detail in order to estimate its effect on the abrasion rate.

4.3 Resultant impact velocity

Auel (2014) proposed a slightly different abrasion model compared to Eq. (10) using the resultant impact velocity V_{im} instead of the vertical velocity W_{im}. Due to that change, additionally the abrasion coefficient k_v was renamed as C_A since it did not represent the value given by Sklar and Dietrich (2004).

A main advantage of using V_{im} is the excellent correlation of both the particle velocity V_p to the Shields parameter given in Eq. (15) and to the particle impact velocity V_{im}. The latter correlation is given in Figure 6 as:

$$\frac{V_{im}}{(gh)^{0.5}} = 1.0\frac{V_p}{(gh)^{0.5}} \qquad R^2 = 1.0 \qquad [26]$$

This reveals, that the impact velocity equals the particle velocity in case of supercritical flows as analyzed in Auel (2014). Consequently, the impact velocity follows in its simplified form using Eq. (16) as:

$$V_p = V_{im} = 20\cdot U_* \qquad \text{[m/s]} \qquad [27]$$

Comparing Eqs. (27) and (20) reveals that the magnitude of the vertical particle impact velocity is 5% of the resultant impact velocity, resulting in an impact angle γ = arcsin(0.05) = 2.9°. Whether applying V_{im} or W_{im} in Eq. (10) consequently leads to quite different results of A_r, if the abrasion coefficient is not adapted accordingly.

A further advantage using the resultant velocity is the different effect of the vertical and horizontal component of the impact velocity. According to Bitter (1963a, b) the vertical component causes the so called *deformation wear*, which is related to the particle impact, whereas the horizontal component causes *cutting wear*, which is related to grinding stress. Engel (1976) stated that erosion depends on the sine of the impact angle because the magnitude of the peak tensile stress varies with the normal component of the impact velocity, i.e. the vertical velocity component is the driving factor. Sklar and Dietrich (2004) stated that cutting wear caused by the horizontal velocity component is only important in ductile materials and in case of highly angular impacting particles, but is not significant when brittle materials are impacted by rounded grains as present in river systems. These statements are confirmed by Auel (2014) stating that the maximum the-

oretical threshold for the energy transferred by sliding and rolling motion is only about 10 and 0.1% of the saltation impact energy, respectively.

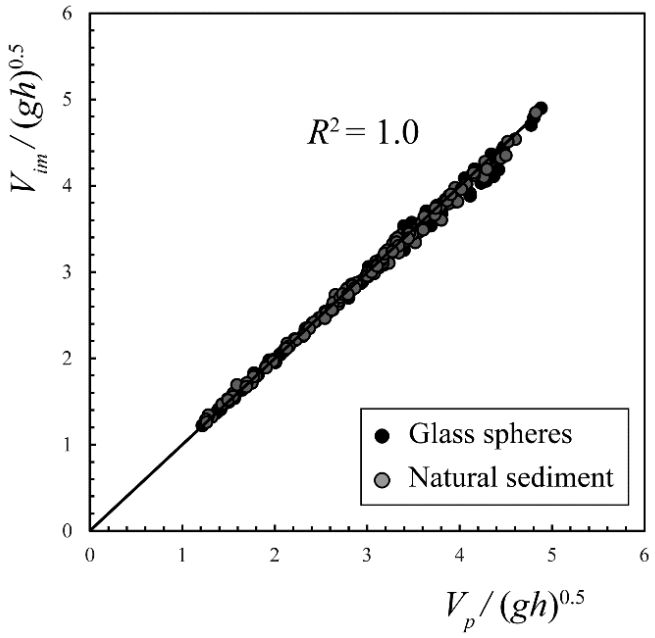

Figure 6: Normalized particle impact velocity V_{im} as a function of normalized particle velocity V_p

Using the resultant impact velocity does not differentiate *deformation* and *cutting* wears but simplifies the applicability of an abrasion model. However, merging these different effects may be also seen as a disadvantage from a physical point of view, as the effects are mixed up. Regardless of the above given explanations, it is proposed to use W_{im} in the saltation-abrasion model given in Eq. (10), for the reasons given hereafter.

The abrasion rate is sensitive to the abrasion coefficient k_v as shown in Section 4.1. Auel (2014) found a linear relation of the measured abraded mass to the supplied sediment mass. However, his proposed abrasion coefficient C_A is only valid in the conducted model study due to the use of the weak mortar (Table 1). The abraded mass of high-performance concrete is expected to be orders of magnitude lower.

So far, the use of the abrasion resistance coefficient k_v as described in Section 3.3 seems to be most adequate. As Sklar and Dietrich (2004) use W_{im} to calculate k_v, the use of W_{im} should be continued as the effect of a slight variation in k_v is already large as described in Section 4.1. An application of V_{im} instead of W_{im} imposes further uncertainties in the estimation of the abrasion rate as V_{im} is 20 times larger than W_{im}. Hence, the use of V_{im} is not meaningful without more knowledge on the underlying abrasion processes resulting from further research on concrete abrasion using standardized abrasion drum/mill facilities as described above.

5 Conclusions

In this contribution the *state of the art* saltation-abrasion model by Sklar and Dietrich (2004) is applied to hydraulic structures exposed to supercritical sediment-laden flows. The proposed model, given in Eq. (10), bases on the particle saltation trajectory, and vertical impact velocity in supercritical flows as well as the invert material properties and the abrasion coefficient k_v. It is shown that

(1) the vertical particle impact velocity equals to the friction velocity and

(2) the abrasion coefficient can be approximated as a first order estimate with a value of $k_v = 10^6$.

The abrasion coefficient k_v is derived from an abrasion rate vs. bed material strength correlation based on standardized abrasion mill experiments. A sensitivity analysis reveals a large effect of k_v on the abrasion rate. Further research is needed to analyze the effects of the parameters i.e. flow velocity, sediment transport rate, particle size, particle hardness, and bed material properties on k_v. Auel (2014) found that the abrasion rate decreases with increasing material strength, but increases with flow velocity and sediment transport rate, and showed that medium-sized particles caused the highest abrasion compared to the smallest and largest particles for the same sediment supply rate. Thus, other parameters directly affect the abrasion, which are not adequately considered by the presented derivation of k_v. Research is currently conducted to quantify a possible correlation between the hydraulic operation conditions, sediment load, invert material properties and measured hydro-abrasion for a wide range of high performance concretes in prototype hydraulic structures (Hagmann *et al.* 2014, 2015). These findings together with data from Mechtcherine *et al.* (2012) and Helbig *et al.* (2012) will enhance the knowledge in concrete abrasion and may be used to find an adequate abrasion coefficient k_v.

Acknowledgments

The first author kindly acknowledges the financial support of the Japanese Society for the Promotion of Science. The financial support of this research project by swisselectric research and the Swiss Federal Office of Energy is also gratefully acknowledged.

Notation

A	area	[m^2]
b	width	[m]
A_r	vertical abrasion rate	[m/s]
A_{rv}	volumetric abrasion rate	[m^3/(sm')]
A_{rg}	gravimetric abrasion rate	[kg/(sm')]

D	particle diameter	[m]
f_c	compression strength	[Pa]
$f_{c,cube}$	compression strength using cubed sample	[Pa]
$f_{c,cyl}$	compression strength using cylindrical sample	[Pa]
f_t	direct tensile strength	[Pa]
f_{tf}	flexure tensile strength	[Pa]
f_{tsp}	splitting tensile strength	[Pa]
g	gravitational acceleration	[m/s^2]
h	flow depth	[m]
H_p	particle saltation height	[m]
I	number of particle impacts per unit length	[1/m].
k_s	equivalent bed roughness height	[m]
k_v	rock resistance coefficient	[-]
L_p	particle saltation length	[m]
P_R	rolling probability	[-]
Q_s	gravimetric bedload rate	[kg/s]
q_s	specific gravimetric bedload rate	[kg/(sm)]
q_s^*	specific gravimetric bedload transport capacity	[kg/(sm)]
R_h	hydraulic radius	[m]
s	density ratio $s = \rho_s/\rho$	[-]
S	energy line slope	[-]
S_b	bed slope	[-]
T^*	transport stage $T^* = \theta/\theta_c$	[-]
U	uniform flow velocity	[m/s]
U_*	friction velocity $U_* = (gR_hS)^{0.5}$	[m/s]
V_p	mean particle velocity	[m/s]
V_S	particle settling velocity	[m/s]
V_{im}	mean resultant particle impact velocity	[m/s]
v_i	particle velocity between two recorded particles	[m/s]
W_{im}	mean vertical particle impact velocity	[m/s]
Y_M	Young's Modulus of elasticity	[Pa]
γ_{im}	particle impact angle	[°]

θ	Shields parameter $\theta = U_*^2/[(s\text{-}1)gD]$	[-]
θ_c	critical Shields parameter	[-]
ρ	fluid density	[kg/m^3]
ρ_c	invert material density	[kg/m^3]
ρ_s	particle density	[kg/m^3]
ω	rotational drum velocity	[rev/min]

References

Auel, C., Albayrak, I., Boes, R.M. (2014a). Turbulence characteristics in supercritical open channel flows: Effects of Froude number and aspect ratio. *Journal of Hydraulic Engineering* 140(4), 04014004, 16p.

Auel, C., Albayrak, I., Boes, R.M. (2014b). Bedload particle velocity in supercritical open channel flows. *Proc. River Flow* (Schleiss et al. eds.), Taylor and Francis, 923-931.

Auel, C. (2014). Flow characteristics, particle motion and invert abrasion in sediment bypass tunnels. *PhD thesis* 22008, also published as *VAW-Mitteilung* 229 (R. Boes, ed.), ETH Zurich, Switzerland.

Auel, C. Boes, R.M. (2011): Sediment bypass tunnel design – review and outlook. *Proc. ICOLD Symposium „Dams under changing challenges"* (A.J. Schleiss & R.M. Boes, eds.), 79th Annual Meeting, Lucerne. Taylor & Francis, London, UK, 403-412.

Arioglu, N., Canan Girin, Z., Arioglu, E. (2006). Evaluation of ratio between splitting tensile strength and compressive strength for concretes up to 120 MPa and its application in strength criterion. *ACI Materials Journal* 103(1), 18–24.

Bitter, J. G. A. (1963a). A study of erosion phenomena, part I. *Wear* 6, 5–1.

Bitter, J. G. A. (1963b). A study of erosion phenomena, part II. *Wear* 6, 169–190.

Boes, R.M., Auel, C., Hagmann, M., Albayrak, I. (2014). Sediment bypass tunnels to mitigate reservoir sedimentation and restore sediment continuity. *Reservoir Sedimentation* (Schleiss, A.J., De Cesare, G., Franca, M.J., Pfister, M., eds.), ISBN 978-1-138-02675-9, Taylor & Francis, London, UK, 221-228.

CEB-FIB (1991). Evaluation of the time dependent behaviour of concrete. *Bulletin d'Information No.* 199, Comité Européen du Béton/Fédération Internationale de la Précontrainte, Lausanne, Switzerland, 201 p.

Chatanantavet, P., Parker, G. (2009). Physically based modeling of bedrock incision by abrasion, plucking, and macroabrasion. *Journal of Geophysical Research: Earth Surface* 114(F04018), 22p.

Clark, S. P. (1966). Handbook of physical constants. *The Geological Society of America*, Memoir 97, 587 p.

Dietrich, W.E. (1982). Settling Velocity of Natural Particles. *Water Resources Research* 18(6), 1615–1626.

EN 1992-1-1 (2004). Eurocode 2: Design of concrete structures - Part 1-1: General rules and rules for buildings. *The European Union per Regulation* 305/2011, Directive 98/34/EC, Directive 2004/18/EC. European Committee for Standardization, Brussels, Belgium.

Engel, P. A. (1976). Impact wear of materials (Tribology). *Elsevier Science Ltd.*, New York.

Ferguson, R.I., Church, M. (2004). A simple universal equation for grain settling velocity. *Journal of Sedimentary Research* 74(6), 933–937.

Hagmann, M., Albayrak, I., Boes, R.M. (2015). Field research: Invert material resistance and sediment transport measurements. Proc. First Int. Workshop on Sediment Bypass Tunnels, *VAW-Mitteilung* 232 (R. Boes, ed.), ETH Zurich, Switzerland.

Hagmann, M., Albayrak, I., Boes, R.M. (2014). Untersuchung verschleissfester Materialien im Wasserbau mit in-situ-Geschiebetransportmessung ('Investigation on wear-resistant materials at hydraulic structures: in-situ measurements of sediment transport and invert abrasion'). Proc. Symposium „Wasserbau und Flussbau im Alpenraum", *VAW-Mitteilung* 227 (R. Boes, ed.), ETH Zürich, Switzerland, 97-106.

Hannant, D. J., Buckley, K. J., Croft, J. (1973). The effect of aggregate size on the use of the cylinder splitting test as a measure of tensile strength. *Materials and Structures* 6(31), 15–21.

Helbig, U., Horlacher, H.-B., Stamm, J., Bellmann, C., Butler, M., Mechtcherine, V. (2012). Nachbildung der Hydroabrasionsbeanspruchung im Laborversuch, Teil 2 – Korrelation mit Verschleiβwerten und Prognoseansätze (Modeling hydroabrasive stress in the laboratory experiment, Part 2 – Correlation with wear values and prognosis approaches). *Bautechnik* 89(5), 320–330 (in German).

Helbig, U., Horlacher, H.-B. (2007). Ein Approximationsverfahren zur rechnerischen Bestimmung des Hydroabrasionsverschleiβes an überströmten Betonoberflächen (An approximation method for the determination of hydroabrasive wear on overflown concrete surfaces). *Bautechnik* 84(12), 854–861 (in German).

Huda, S.A., Small, E.E. (2014). Modeling the effects of bed topography on fluvial bedrock erosion by saltating bed load. *Journal of Geophysical Research: Earth Surface* 119, 1222–1239.

Ishibashi, T. (1983). Hydraulic study on protection for erosion of sediment flush equipments of dams. *Civil Society Proc*. 334(6), 103–112 (in Japanese).

Jacobs, F., Winkler, K., Hunkeler, F., Volkart, P. (2001). Betonabrasion im Wasserbau (Concrete abrasion in hydraulic structures). *VAW-Mitteilung* 168 (H.-E. Minor, ed.), ETH Zurich, Switzerland (in German).

Johnston, I. W. (1985). Strength of intact geomechanical materials. *Journal of Geotechnical Engineering ASCE* 111(6) 730–748.

Lamb, M.P., Dietrich, W.E., Sklar, L.S. (2008). A model for fluvial bedrock incision by impacting suspended and bed load sediment. *Journal of Geophysical Research* 113(F03025), 18p.

Mechtcherine, V., Bellmann, C., Helbig, U., Horlacher, H.-B., Stamm, J. (2012). Nachbildung der Hydroabrasionsbeanspruchung im Laborversuch, Teil 1 – Experimentelle Untersuchungen zu Schädigungsmechanismen im Beton (Modeling hydroabrasive stress in the laboratory experiment, Part 1 – experimental investigations of damage mechanisms in concrete). *Bautechnik* 89(5), 309–319 (in German).

Noguchi, T., Tomosawa, F., Nemati, K.M., Chiaia, B.M., Fantilli, A.P. (2009). A practical equation for elastic modulus of concrete. *ACI Structural Journal* 106(5), 690–696.

Rocco, C., Guinea, G.V., Planas, J., Elices, M. (1999). Size effect and boundary conditions in the Brazilian test: theoretical analysis. *Materials and Structures* 32, 437–444.

Scheingross, J.S., Brun, F., Lo, D.Y., Omerdin, K., Lamb, M.P. (2014). Experimental evidence for fluvial bedrock incision by suspended and bedload sediment. *Geology* 42(6), 523–526.

Setunge, S., Attard, M.M., Darvall, P.P. (1993). Ultimate strength of confined very high-strength concretes. *ACI Structural Journal* 90(6) 632–641.

Sklar, L.S., Dietrich, W.E. (2012). Correction to "A mechanistic model for river incision into bedrock by saltating bed load". *Water Resources Research* 48(W06902), 2p.

Sklar, L.S., Dietrich, W.E. (2006). The role of sediment in controlling steady-state bedrock channel slope: Implications of the saltation–abrasion incision model. *Geomorphology* 82, 58–83.

Sklar, L.S., Dietrich, W.E. (2004). A mechanistic model for river incision into bedrock by saltating bed load. *Water Resources Research* 40(W06301), 21p.

Sklar, L.S., Dietrich, W.E. (2001). Sediment and rock strength controls on river incision into bedrock. *Geology* 29(12), 1087–1090.

Sklar, L.S., Dietrich, W.E. (1998). River longitudinal profiles and bedrock incision models: Stream power and the influence of sediment supply. *Geophysical Monograph* 107, American Geophysical Union, 237–260.

Sumi, T., Okano, M., Takata, Y. (2004). Reservoir sedimentation management with bypass tunnels in Japan. *Proc. 9th International Symposium on River Sedimentation*, Yichang, China, 1036–1043.

Turowski, J.M., Böckli, M., Rickenmann, D., Beer A.R. (2013). Field measurements of the energy delivered to the channel bed by moving bed load and links to bedrock erosion. *Journal of Geophysical Research: Earth Surface* 118, 2438–2450.

Turowski, J.M. (2009). Stochastic modeling of the cover effect and bedrock abrasion. *Water Resources Research* 45(W03422), 13p.

Turowski, J.M., Lague, D., Hovius, N. (2007). Cover effect in bedrock abrasion: A new derivation and its implications for the modeling of bedrock channel morphology. *Journal of Geophysical Research: Earth Surface* 112, F04006, 16p.

Authors

Dr. Christian Auel (corresponding Author)*
Prof. Dr. Tetsuya Sumi
Water Resources Research Center, Disaster Prevention Research Institute, Kyoto University, Japan
Email: christian.auel@alumni.ethz.ch

Dr. Ismail Albayrak
Prof. Dr. Robert M. Boes
Laboratory of Hydraulics, Hydrology and Glaciology (VAW), ETH Zurich, Switzerland

* formerly VAW, ETH Zurich, Switzerland